Acta Crystallographica Section F
Structural Biology and Crystallization Communications
ISSN 1744-3091

Natalie Zeytuni and Raz Zarivach*

Department of Life Sciences and National Institute for Biotechnology in the Negev, Ben Gurion University of the Negev, PO Box 653, Beer-Sheva 84105, Israel

Correspondence e-mail: zarivach@bgu.ac.il

Received 6 April 2010
Accepted 17 May 2010

Crystallization and preliminary crystallographic analysis of the *Magnetospirillum magneticum* AMB-1 and *M. gryphiswaldense* MSR-1 magnetosome-associated proteins MamA

MamA is a unique magnetosome-associated protein that is predicted to contain six sequential tetratricopeptide-repeat (TPR) motifs. The TPR structural motif serves as a template for protein–protein interactions and mediates the assembly of multi-protein complexes. Here, the crystallization and preliminary X-ray analysis of recombinant and purified *Magnetospirillum magneticum* and *M. gryphiswaldense* MamA are reported for the first time. *M. gryphiswaldense* MamAΔ41 crystallized in the tetragonal space group $P4_12_12$ or $P4_32_12$, with unit-cell parameters $a = b = 58.88$, $c = 144.09$ Å. *M. magneticum* MamAΔ41 crystallized in the orthorhombic space group $P2_12_12_1$, with unit-cell parameters $a = 44.75$, $b = 76.19$, $c = 105.05$ Å. X-ray diffraction data were collected to resolutions of 2.0 and 1.95 Å, respectively.

1. Introduction

The tetratricopeptide repeat (TPR) is a structural motif that is found in a wide range of proteins as an independent fold or as a segment of a fold and serves as a template for protein–protein interactions that can mediate the assembly of multi-protein complexes (D'Andrea & Regan, 2003). TPRs are thus involved in many different processes in a eukaryotic cell, including synaptic vesicle fusion (Young *et al.*, 2003), peroxisomal targeting and import (Brocard & Hartig, 2006; Fransen *et al.*, 2008) and mitochondrial and chloroplast import (Baker *et al.*, 2007; Mirus *et al.*, 2009). In addition, TPRs are required for many bacterial pathways involving outer membrane assembly (Gatsos *et al.*, 2008) and pathogenesis (Tiwari *et al.*, 2009; Edqvist *et al.*, 2006). One unique bacterial system that requires TPR proteins is the magnetosome of magnetotactic bacteria.

Magnetotactic bacteria comprise a diverse group of aquatic microorganisms that have the unique ability to navigate along geomagnetic fields, a behaviour that is believed to simplify their search for transition environments such as the oxic–anoxic transition zone (Faivre & Schuler, 2008). In these microorganisms, the biomineralization of iron takes place in the magnetosome, a specialized subcellular organelle that is assembled from a chain of bilayer lipid vesicles that each induce the deposition of, and enclose an ~50 nm crystal of, magnetite or its sulfide analogue greigite (Fe_3S_4). This organelle is characterized by its ability to essentially grow one magnetite crystal per vesicle under ambient conditions.

Magnetosome formation and magnetite biomineralization are controlled by a large set of proteins that includes unique soluble and integral membrane proteins (Schuler, 2008; Murat *et al.*, 2010). Comparison of magnetospirillum species (*i.e.* *Magnetospirillum magneticum* AMB-1, *M. magnetotacticum* MS-1 and *M. gryphiswaldense* MSR-1) has shown that genes encoding magnetosome proteins are situated on a single genomic island that contains four main operons, termed *mamAB*, *mamCD*, *mms6* and *mamXY* (Jogler, Kube *et al.*, 2009). Deletion of the magnetosome-related genomic island from the genome results in loss of magnetic orientation (Bazylinski & Frankel, 2004; Komeili, 2007). Studies of magnetosome-forming genes have revealed that the biomineralization process is controlled

by these four operons, with the *mamAB* operon being assumed to be involved in iron transport and magnetosome-vesicle alignment (Scheffel *et al.*, 2008; Amemiya *et al.*, 2007; Schuler, 2008; Komeili, 2007). Accordingly, the sequencing of additional magnetotactic bacterial genomes revealed a high degree of conservation within the *mamAB* operon (Schubbe *et al.*, 2009; Matsunaga *et al.*, 2009; Jogler, Kube *et al.*, 2009; Jogler, Lin *et al.*, 2009).

One of the most highly conserved magnetosome-associated proteins is MamA (also known as Mms24 and Mam22). Copurification of MamA with magnetosome vesicles indicated that MamA accounts for ∼10% of the magnetosome-associated proteins (Grunberg *et al.*, 2004); while deletion of MamA does not affect vesicle formation, it does result in the appearance of shorter magnetosome chains, thereby limiting iron accumulation (Komeili *et al.*, 2004). MamA is targeted to the magnetosomal matrix (Taoka *et al.*, 2006). Moreover, complementation of a Δ*mamA* mutant with green-fluorescent-protein-tagged MamA showed the protein to be localized to the magnetosome during the logarithmic but not the stationary phase of growth (Komeili *et al.*, 2004). However, the role of MamA in magnetosome function remains unresolved.

To analyze the structure–function relationship of MamA and to elucidate structure-based differences between *Magnetospirillum* magnetotactic bacterial species, we have initiated crystallographic studies of the MamA protein from *M. magneticum* AMB-1 and *M. gryphiswaldense* MSR-1. Here, we report the crystallization and preliminary X-ray analysis of a truncated version of MamA (MamAΔ41).

2. Materials and methods

2.1. Expression of the *mamAΔ41* gene in *Escherichia coli*

The truncated *mamAΔ41* gene was amplified using the polymerase chain reaction (PCR) from the genomic DNA of two species of magnetotactic bacteria, *i.e. M. magneticum* AMB-1, using the primers AMB-1-f, 5′-GCATTACGCATATGGACGACATCCGCCAGGTG-3′, and AMB-1-r, 5′-GCGCGGCAGCCATATGGCATACG-3′, and *M. gryphiswaldense* MSR-1, using the primers MSR-1-f, 5′-GCATTACGCATATGGATGACATTCGTCAGGTGTATTACCG-3′, and MSR-1-r, 5′-GCGCGGCAGCCATATGGCATACG-3′. The primers were designed to introduce an *Nco*I site at the initiation codon, ATG, followed by a glycine-encoding codon (GGA) to maintain the reading frame. The termination codon was replaced by an *Sco*I site. The fragments were digested with *Nco*I and *Sac*I and cloned into the respective sites of plasmid pET52b(+), giving rise to plasmids pET52bMamAΔ41-MSR1 and pET52bMamAΔ41-AMB1. In these constructs, the *mamAΔ41* genes were fused in-frame to express a His_{10} tag at the C-terminus of the protein.

E. coli strain BL21 harbouring plasmid pET52bMamAΔ41 were grown in auto-induction medium (Studier, 2005) containing ampicillin (50 mg ml^{-1}) at 310 K for 3 h. The cultivation temperature was then shifted from 310 to 300 K for a further 48 h. The cells were harvested by centrifugation at 5465*g* for 10 min at 277 K.

2.2. Purification of MamAΔ41

MamAΔ41-MSR-1-expressing cells were suspended in buffer *A* (20 m*M* Tris–HCl pH 8, 1 *M* NaCl, 20 m*M* imidazole) and incubated with DNase I (1 mg ml^{-1}) and EDTA-free protease-inhibitor cocktail (P8849, Sigma) for 20 min at 277 K. The cells were then disrupted by two cycles in a French press pressure cell at 172 MPa. Cell debris was separated by centrifugation at 270 000*g* for 1 h at 277 K and the soluble fraction was applied onto a home-made gravity Ni–NTA column (4 ml bed volume, 2.5 cm diameter; Econo-Column Chromatography Columns from Bio-Rad containing Ni–NTA His-Bind Resin, Lot M0063428 from Novagen) pre-equilibrated with buffer *A*. The protein was washed with 100 ml buffer *B* (20 m*M* Tris–HCl pH 8, 1 *M* NaCl, 40 m*M* imidazole) and and eluted with buffer *C* (20 m*M* Tris–HCl pH 8, 5 m*M* NaCl and 500 m*M* imidazole). To remove the His_{10} tag, bovine thrombin (10 U ml^{-1}; 9002-04-4, Fisher Bio Reagents) was added to the eluted protein and the mixture was dialyzed against buffer *D* (10 m*M* Tris–HCl pH 8, 5 m*M* NaCl) for 16 h at 277 K. The protein was applied onto a MonoQ column (4.6/100 PE, GE Healthcare Biosciences) equilibrated with buffer *E* (10 m*M* Tris–HCl pH 8, 40 m*M* NaCl) and eluted with a linear gradient of 40–1000 m*M* NaCl in buffer *C*. The relevant protein peak was collected and dialyzed against buffer *D* for 4 h at 277 K. The protein was concentrated to a concentration of 8 mg ml^{-1} using a Vivaspin-4 (10 000 molecular-weight cutoff; Sartorius Stedim Biotech GmbH) and then applied onto a size-exclusion column (HiLoad 26/60 Superdex 200, GE Healthcare Biosciences) equilibrated with buffer *D*. Purified MamAΔ41-MSR1 was then concentrated to 17.0 mg ml^{-1} for crystallization, flash-frozen in liquid nitrogen and stored at 193 K. The sample purity at this stage was analyzed by SDS–PAGE and protein identification was confirmed by tandem mass spectroscopy. The purification of MamAΔ41-AMB1 was similar to that of MamAΔ41-MSR1 with small modifications to the NaCl concentrations, as described elsewhere (Zeytuni & Zarivach, 2010).

2.3. Crystallization

MamAΔ41 was crystallized using the sitting-drop vapour-diffusion method at 286 K. 0.5 µl MamAΔ41 (AMB-1, 20 mg ml^{-1}; MSR-1, 17 mg ml^{-1}) and 0.5 µl reservoir solution were mixed to form the drop. The initial crystallization conditions were examined using commercial screening kits from Hampton Research (Crystal Screen 1, Crystal Screen 2, Index and PEG/Ion Screen), Emerald BioSystems (Cryo I and Wizard I and II) and Molecular Dimensions (Structure Screen I and II and ProPlex).

2.4. Diffraction data collection

Crystals were harvested and flash-cooled in liquid nitrogen without addition of cryoprotecting solution. Diffraction data were collected on beamline ID14-2 of the ESRF (Grenoble, France), which is equipped with an ADSC Q4 CCD detector. Data collection was performed at 100 K. For the MamAΔ41 (MSR-1) data set, a total of 360 frames were collected with an oscillation range of 1° and an exposure time of 8 s per image. The crystal-to-detector distance was 155 mm. For the MamAΔ41 (AMB-1) data set, a total of 180 frames were collected with an oscillation range of 1° and an exposure time of 8 s per image. The crystal-to-detector distance was 160 mm. The data were processed using *MOSFLM* (Leslie, 2003), *POINTLESS* (Evans, 2006) and *SCALA* from the *CCP*4 program suite (Collaborative Computational Project, Number 4, 1994).

3. Results and discussion

The secondary-structure model suggested by Okuda & Fukumori (2001) for AMB-1 MamA shows that the putative TPR motif in the N-terminal region of the protein contains amphiphilic residues. We have constructed a secondary-structure and sequence alignment based on protein-homology models found using the *HH-Pred* server (http://toolkit.tuebingen.mpg.de/hhpred). The final models were built according to the top seven previously determined structures. Although these templates are highly similar in secondary structure

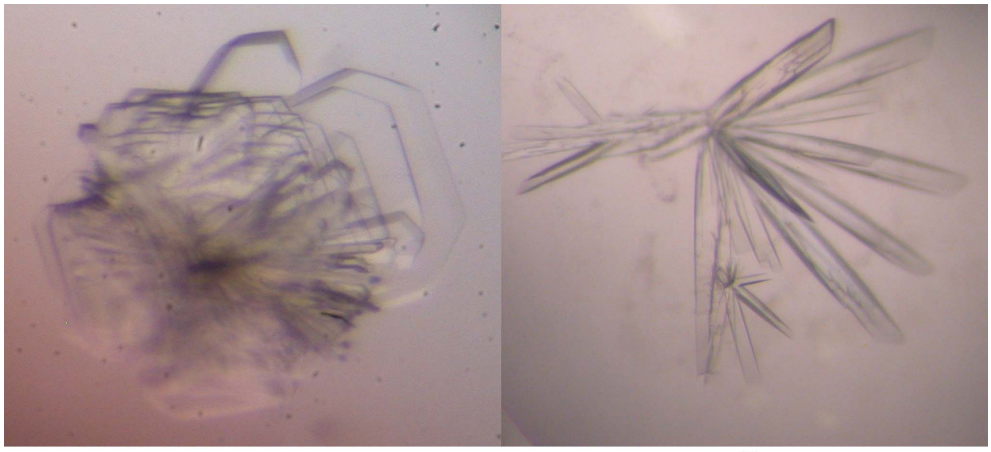

(*a*) (*b*)

Figure 1
Micrographs of (*a*) the MamAΔ41 MSR-1 and (*b*) the MamAΔ41 AMB-1 crystals.

Table 1
Diffraction data and processing statistics.

Values in parentheses are for the highest resolution shell.

	MamAΔ41 MSR-1	MamAΔ41 AMB-1
Beamline	ID14-2, ESRF	ID14-2, ESRF
Space group	$P4_12_12$ or $P4_32_12$	$P2_12_12_1$
Unit-cell parameters (Å, °)	$a = b = 58.88$, $c = 144.09$, $\alpha = \beta = \gamma = 90$	$a = 44.75$, $b = 76.19$, $c = 105.05$, $\alpha = \beta = \gamma = 90$
Resolution (Å)	17.00–2.00 (2.03–2.00)	20.00–1.95 (1.98–1.95)
Reflections, total	325644	179857
Reflections, unique	17139	26835
R_{merge}† (%)	9.2 (60.7)	6.5 (23.9)
$I/\sigma(I)$	50.0 (6.15)	45.45 (4.77)
Completeness (%)	96.0 (93.6)	99.7 (99.8)
Redundancy	19	6.7
Wavelength (Å)	0.933	0.933

† $R_{merge} = \sum_{hkl}\sum_i |I_i(hkl) - \langle I(hkl)\rangle| / \sum_{hkl}\sum_i I_i(hkl)$, where $I_i(hkl)$ is the observed intensity of an individual reflection and $\langle I(hkl)\rangle$ is the mean intensity of that reflection.

(overall E value of $>1 \times 10^{-30}$), their sequence identity to MamAΔ41 is significantly lower, in the range 20–30%. These seven templates were PDB entries 3cv0 (peroxisomal targeting signal 1 receptor PEX5; Sampathkumar *et al.*, 2008), 1fch (peroxisomal targeting signal 1 receptor; Gatto *et al.*, 2000), 2q7f (YrrB protein; Han *et al.*, 2007), 2pl2 (hypothetical conserved protein TTC0263; Lim *et al.*, 2007), 2ho1 (type 4 fimbrial biogenesis protein, PilF; J. Koo, L. Sampaleanu, P. Yip, S.-Y. Ku, D. Neculai, A. Yu, L. L. Burrows & P. L. Howell, unpublished work), 1w3b (O-linked GlcNAc transferase; Jinek *et al.*, 2004) and 2gw1 (mitochondrial precursor protein import receptor; Wu & Sha, 2006). These models also suggest that MamA contains six sequential TPR motifs which create a superhelix-like structure. Furthermore, a general search of the PDB revealed that TPR-containing proteins were only able to crystallize after deletion of the N-terminal extensions. Taking these findings into consideration, we decided to delete the putative TPR repeat corresponding to the first 40 amino acids. Subsequently, we were able to purify and crystallize MamAΔ41 from both species (Fig. 1).

MamAΔ41 from both species was expressed in *E. coli* and purified to homogeneity, with a yield of approximately 60 mg purified protein from 60 g bacterial culture. MamAΔ41 (MSR-1) crystals appeared using Index condition No. 5 (2 *M* ammonium sulfate, 0.1 *M* HEPES pH 7.5). These conditions were further refined and resulted in MamAΔ41 (MSR-1) crystals that were grown with altered reservoir conditions (1.65 *M* ammonium sulfate, 0.1 *M* HEPES pH 8.2, 0.1 m*M* NaCl). MamAΔ41 (AMB-1) crystals appeared using Index condition No. 85 [0.2 *M* magnesium chloride, 0.1 *M* Tris–HCl pH 8.5, 25%(*w*/*v*) PEG 3350]. These conditions were further refined and MamAΔ41 (AMB-1) crystals were grown with altered reservoir conditions [0.1 *M* magnesium chloride, 0.1 *M* Tris–HCl pH 8.5, 25%(*w*/*v*) PEG 3350].

Crystals of MamAΔ41 (MSR-1) were reproducibly obtained in space group $P4_12_12$ or $P4_32_12$, which are enantiomorphic space groups that both fulfil the systematic absence rules. Further validation of the chosen space groups was perform by *POINTLESS*, which indicated that the space-group choices were correct, with a symmetry-absence probability of 0.885 each. The unit-cell parameters were $a = b = 58.88$, $c = 144.09$ Å (Table 1), with diffraction to a resolution of 2.0 Å. Assuming the presence of one monomer per asymmetric unit, the calculated V_M value (Matthews, 1968) and solvent content were 3.12 Å^3 Da^{-1} and 60.59%, respectively, both of which are within the normal range of values observed for soluble protein crystals. Crystals of MamAΔ41 (AMB-1) were reproducibly obtained in space group $P2_12_12_1$ (*POINTLESS* symmetry-absence probability of 0.908 and total probability of 0.898), with unit-cell parameters a = 44.75, b = 76.19, c = 105.05 Å (Table 1), with diffraction to a resolution of 1.95 Å. Assuming the presence of two monomers per asymmetric unit, the calculated V_M value (Matthews, 1968) and solvent content are 2.24 Å^3 Da^{-1} and 45.06%, respectively.

MamA is the first magnetosome-associated protein as well as the first TPR-containing protein from magnetotactic bacteria to be crystallized and will lead to the determination of the first magnetosome-associated protein structure. These crystals should be sufficient for structural determination, as they diffracted to high resolution and yielded data sets with a low R_{merge} and high redundancy. To determine the structure and to differentiate between the two possible tetragonal space groups, molecular-replacement methodologies will be applied. For this protocol, the constructed homology models and TPR-containing protein structures will be used. Such molecular-replacement experiments are ongoing.

References

Amemiya, Y., Arakaki, A., Staniland, S. S., Tanaka, T. & Matsunaga, T. (2007). *Biomaterials*, **28**, 5381–5389.
Baker, M. J., Frazier, A. E., Gulbis, J. M. & Ryan, M. T. (2007). *Trends Cell Biol.* **17**, 456–464.
Bazylinski, D. A. & Frankel, R. B. (2004). *Nature Rev. Microbiol.* **2**, 217–230.
Brocard, C. & Hartig, A. (2006). *Biochim. Biophys. Acta*, **1763**, 1565–1573.

Collaborative Computational Project, Number 4 (1994). *Acta Cryst.* D**50**, 760–763.
D'Andrea, L. D. & Regan, L. (2003). *Trends Biochem. Sci.* **28**, 655–662.
Edqvist, P. J., Broms, J. E., Betts, H. J., Forsberg, A., Pallen, M. J. & Francis, M. S. (2006). *Mol. Microbiol.* **59**, 31–44.
Evans, P. (2006). *Acta Cryst.* D**62**, 72–82.
Faivre, D. & Schuler, D. (2008). *Chem. Rev.* **108**, 4875–4898.
Fransen, M., Amery, L., Hartig, A., Brees, C., Rabijns, A., Mannaerts, G. P. & Van Veldhoven, P. P. (2008). *Biochim. Biophys. Acta*, **1783**, 864–873.
Gatsos, X., Perry, A. J., Anwari, K., Dolezal, P., Wolynec, P. P., Likic, V. A., Purcell, A. W., Buchanan, S. K. & Lithgow, T. (2008). *FEMS Microbiol. Rev.* **32**, 995–1009.
Gatto, G. J. Jr, Geisbrecht, B. V., Gould, S. J. & Berg, J. M. (2000). *Nature Struct. Biol.* **7**, 1091–1095.
Grunberg, K., Muller, E. C., Otto, A., Reszka, R., Linder, D., Kube, M., Reinhardt, R. & Schuler, D. (2004). *Appl. Environ. Microbiol.* **70**, 1040–1050.
Han, D., Oh, J., Kim, K., Lim, H. & Kim, Y. (2007). *Biochem. Biophys. Res. Commun.* **360**, 784–790.
Jinek, M., Rehwinkel, J., Lazarus, B. D., Izaurralde, E., Hanover, J. A. & Conti, E. (2004). *Nature Struct. Mol. Biol.* **11**, 1001–1007.
Jogler, C., Kube, M., Schubbe, S., Ullrich, S., Teeling, H., Bazylinski, D. A., Reinhardt, R. & Schuler, D. (2009). *Environ. Microbiol.* **11**, 1267–1277.
Jogler, C., Lin, W., Meyerdierks, A., Kube, M., Katzmann, E., Flies, C., Pan, Y., Amann, R., Reinhardt, R. & Schuler, D. (2009). *Appl. Environ. Microbiol.* **75**, 3972–3979.
Komeili, A. (2007). *Annu. Rev. Biochem.* **76**, 351–366.
Komeili, A., Vali, H., Beveridge, T. J. & Newman, D. K. (2004). *Proc. Natl Acad. Sci. USA*, **101**, 3839–3844.
Leslie, A. G. W. (2003). *MOSFLM* v.6.2.3. MRC Laboratory of Molecular Biology, Cambridge, England.
Lim, H., Kim, K., Han, D., Oh, J. & Kim, Y. (2007). *Mol. Cell*, **24**, 27–36.
Matsunaga, T., Nemoto, M., Arakaki, A. & Tanaka, M. (2009). *Proteomics*, **9**, 3341–3352.
Matthews, B. W. (1968). *J. Mol. Biol.* **33**, 491–497.
Mirus, O., Bionda, T., von Haeseler, A. & Schleiff, E. (2009). *J. Mol. Model.* **15**, 971–982.
Murat, D., Quinlan, A., Vali, H. & Komeili, A. (2010). *Proc. Natl Acad. Sci. USA*, **107**, 5593–5598.
Okuda, Y. & Fukumori, Y. (2001). *FEBS Lett.* **491**, 169–173.
Sampathkumar, P., Roach, C., Michels, P. A. & Hol, W. G. J. (2008). *J. Mol. Biol.* **381**, 867–880.
Scheffel, A., Gardes, A., Grunberg, K., Wanner, G. & Schuler, D. (2008). *J. Bacteriol.* **190**, 377–386.
Schubbe, S., Williams, T. J., Xie, G., Kiss, H. E., Brettin, T. S., Martinez, D., Ross, C. A., Schuler, D., Cox, B. L., Nealson, K. H. & Bazylinski, D. A. (2009). *Appl. Environ. Microbiol.* **75**, 4835–4852.
Schuler, D. (2008). *FEMS Microbiol. Rev.* **32**, 654–672.
Studier, F. (2005). *Protein Expr. Purif.* **41**, 207–234.
Taoka, A., Asada, R., Sasaki, H., Anzawa, K., Wu, L.-F. & Fukumori, Y. (2006). *J. Bacteriol.* **188**, 3805–3812.
Tiwari, D., Singh, R. K., Goswami, K., Verma, S. K., Prakash, B. & Nandicoori, V. K. (2009). *J. Biol. Chem.* **284**, 27467–27479.
Wu, Y. & Sha, B. (2006). *Nature Struct. Mol. Biol.* **13**, 589–593.
Young, J. C., Barral, J. M. & Hartl, F. U. (2003). *Trends Biochem. Sci.* **28**, 541–547.
Zeytuni, N. & Zarivach, R. (2010). *J. Vis. Exp.* **37**, doi:10.3791/1844.